On the Structure of Dissolving Thin Liquid Films

D. G. SUCIU

Research Center of Organic Chemistry of the Romanian Academy, Bucharest, Romania

OCTAVIAN SMIGELSCHI and ELI RUCKENSTEIN

Polytechnical Institute, Bucharest, Romania

The structure of thin circular films, formed over a flat water surface during the dissolving (influenced by surface forces) of isobutanol, is examined by performing film thickness and surface velocity measurements. The thicknesses were obtained by light absorption determinations, and the velocities by a stroboscopic method. The film profiles and the dynamic wetting angles obtained differ markedly from those corresponding to a static lens. This is explained by considering the equilibrium between dynamic surface tensions instead of that between static surface tensions.

In a previous paper (*1*) the quasisteady dissolving of a thin liquid film fed continuously from a point source on a flat water surface was examined. It was observed that for many organic substances, the film had a definite contour, its structure depending on the nature of the liquid used, and on its flow rate. Macroscopically, the liquid film appeared to have a constant thickness and also to end abruptly at the contour. The surface velocity appeared also to vary discontinuously at the film contour.

It was our intention to clarify the actual structure of the film, especially in the region near the contour and for this reason measurements concerning the film thickness and velocity were carried out. The measurements also enable one to obtain information concerning the liquid-liquid contact angle in dynamical conditions.

EXPERIMENTAL PROCEDURE

Film Thickness Measurements

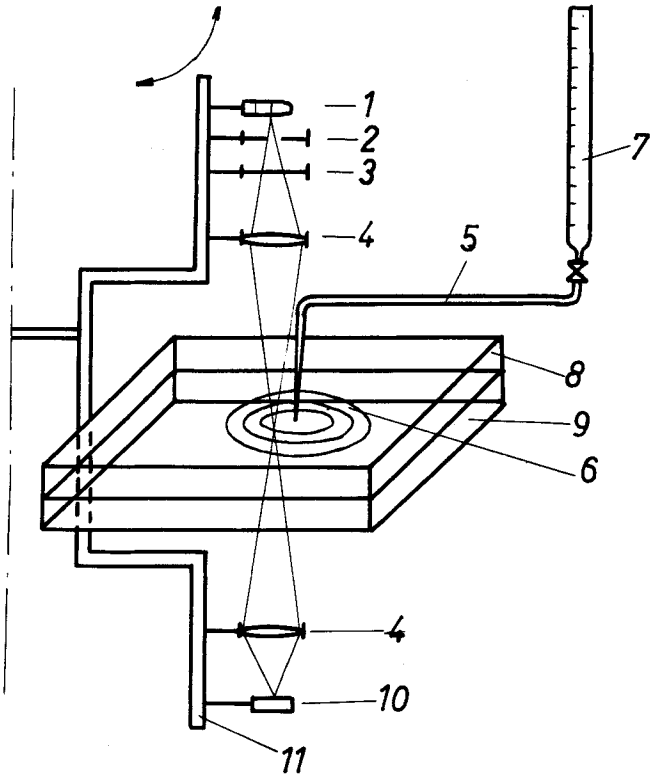

Fig. 1. Arrangement for film thickness measurements. 1. mercury vapor lamp; 2. slit; 3. filter; 4. lens; 5. capillary; 6. liquid film; 7. burette; 8. dish; 9. water layer; 10. photo-cell; 11. yoke.

In principle, this method consists of determining the absorption suffered by a monochromatic beam of light while it passed through the liquid film into which a suitable absorbing substance was previously dissolved.

The arrangement is shown in Figure 1. Into a polymethylmethacrylate prismatic dish, of 500 × 500 and 150 mm. high, about 20 liter tap water were introduced. The films to be studied were formed, as in (*1*), by feeding isobutanol with constant flow rates through a glass capillary, placed in the central part and immediately above the extended, flat, and otherwise stagnant water surface. The film diameter was controlled by adjusting the isobutanol flow rate. Quasisteady conditions were achieved by keeping the ratio between the amount of water used, and that of isobutanol fed during an experiment greater than 2,000.

The vertically aligned optical system consisted of a mercury vapour 100 w. lamp, a slit, a filter (transparent for radiations with wavelengths above 545 mμ), two lenses, and a photoresistive cell. The upper lens focused the filtered light beam on the film, while the lower lens focused the beam emerging from the film on the photocell. All components of the optical system were fastened on a rigid yoke which could rotate around a vertical axis. In this manner, the focused light beam could travel along the diameter of the stationary film.

The photocell (sensitivity 6,000 μa/lumen × v.) was powered with 100 to 200 v. d.c. and the through current was measured by means of a mirror galvanometer having a sensitivity of 10^{-9} amp./scale division.

Since the maximum sensitivity of the photocell was for wave lengths of about 600 mμ, gentian violet (methyl violet) was dissolved in the isobutanol in order to increase the absorption power of the film. This substance has a strong absorption maximum at 576 mμ; besides it is well dissolved by both isobutanol and water, and in acid medium becomes practically colorless. Separate determinations have shown that the gentian violet, in the concentration used here, does not affect the relationship of film diameter vs. flow rate obtained in (*1*). It is therefore reasonable to assume that this substance will not modify the film profile. The water in the dish was acidulated with hydrochloric acid so as to form a 0.5-1% by weight solution. In this manner, the gentian violet dissolving in the water together with the isobutanol loses its color and does not interfere with the film thickness measurements. The use of diluted hydrochloric acid solution instead of tap water does not affect the film diameter vs. isobutanol flow rate relationship, and the film thickness, as ascertained by performing duplicate measurements with and without using hydrochloric acid (the latter at very short durations in order to avoid the dissolving in water of a too large amount of gentian violet). The conversion of the extinction values into film thickness values was made by means of a calibration curve obtained by using precision quartz cuvettes filled with colored isobutanol.

Film velocity measurements

The dish, capillary, and burette were the same as above. On

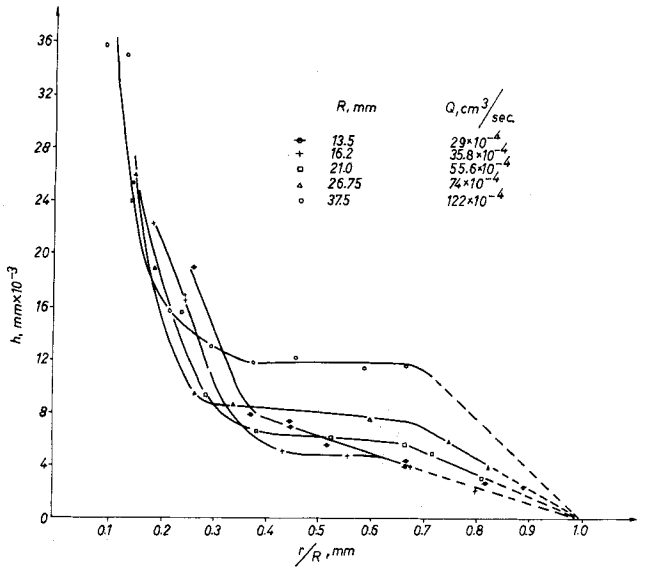

Fig. 2. Film thicknesses vs. r/R for various flow rates

the film, as near the capillary as possible, tracers (tin foil disks, 0.3 mm. diameter and 0.01 mm. thick, having good light reflecting properties) were placed, and their radial movement was photographed by means of an Exacta Varex camera, placed above the capillary.

Between the camera and the film, a blackened aluminium disk with a 20 cm. diameter and having a slot sector over 36 deg. of arc was rotated at a suitable known and constant speed. The camera shutter was set at 3 sec. exposure time, and a tracer was placed on the film. The tracer was viewed by the photographic film only when the disk slot was in front of the camera's objective. The desired illumination was achieved by using three 100 w. mirror bulbs.

In this manner a series of images of the tracer travelling across the film were obtained on the same photograph. The distances between the capillary and the successive images of the tracer, read on the positives, were plotted vs. time (obtained from the known rotation velocity of the slotted disk). Each of the velocity values reported here represents the slope of this curve (obtained graphically) in the points corresponding to the indicated r/R values. Tabulated primary and derived data are given elsewhere (2).

RESULTS

In Figure 2 the film thickness vs. r/R is shown for various flow rates. The film radius R is univocally related to the flow-rate of isobutanol (1).

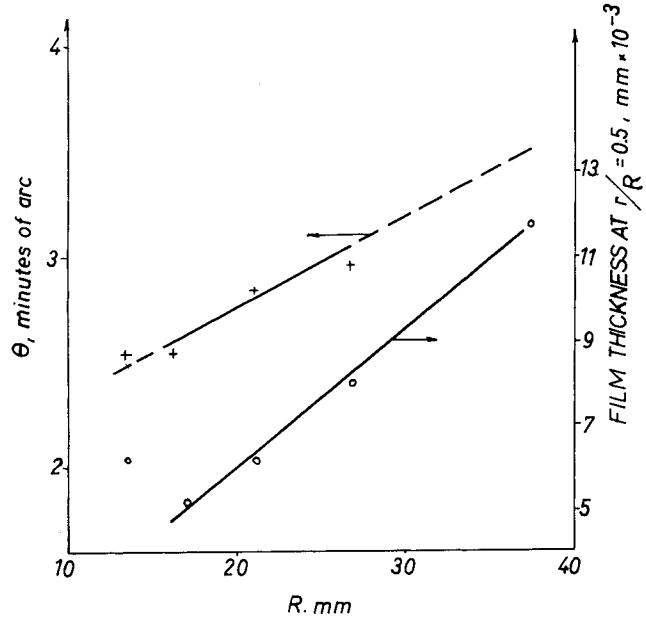

Fig. 3. Contact angles at $r/R = 1$ and film thickness at $r/R = 0.5$.

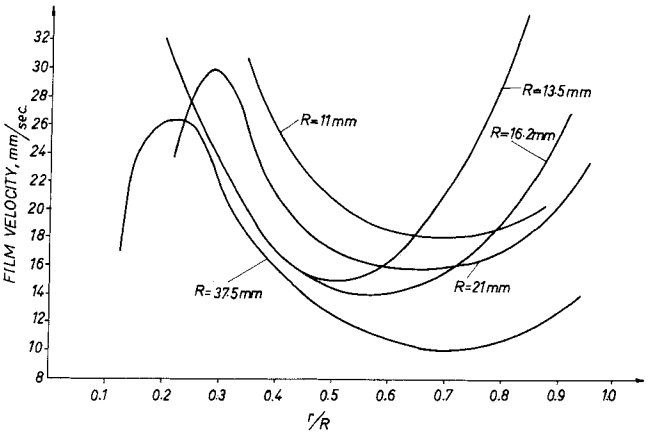

Fig. 4. Film velocity vs. r/R at various flow rates.

Three regions may be noted. In the first region (near the capillary) the thickness decreases rapidly, it becomes practically constant in the middle region, and decreases again gradually, near the film contour in the third (border) region. No constant thickness region is observed however in the film of 13.5 mm. radius. It seems that the capillary and wetting forces (which act on the form of the film in the initial and border regions respectively) extend, for this small radius, their influence over the whole film.

The angle made by the film surface and the water-isobutanol interface in the vicinity of the contour, as determined from Figure 2 is represented in Figure 3, together with the film thickness in the middle region. Concerning the contact angle values given in Figure 3, one may note that only three of the five curves of Figure 2 have points (which seem reliable) in the range $0.65 < r/R < 1$. Therefore, though the θ vs. R dependence shown in Figure 3 may be debatable, nevertheless the order of magnitude of the contact angles obtained for these dynamic conditions, is to be noted.

Film velocities are given in Figure 4* vs. r/R. Though the curves corresponding to a given flow rate (Figure 5) show that the measurements are only moderately reproducible, their shapes are quite similar.

The individual v values for a given r/R may differ from their arithmetical mean by as much as 50%. As seen from Figure 5, these deviations are due largely to the fact that the curves, otherwise similar in shape, seem to have suffered different translations both (a) along the v axis and (b) along the r/R axis.

(a) Since the tracer is wetted by isobutanol, it will not necessarily float at the air-film interface during its radial motion but, since parts of it may be submerged in the

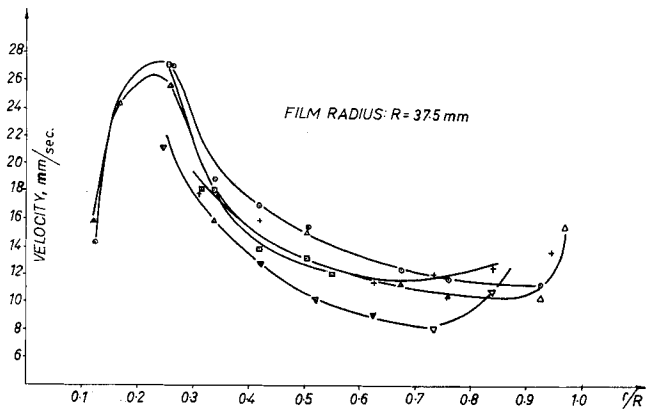

Fig. 5. Film velocities vs. r/R, for $R = 37.5$ mm.

* Each of the curves of Figure 4 was obtained as arithmetical mean of 2-5 series of v vs. r/R experimental determinations. For reasons of clarity and since the curves in Figure 4 are intended to have only qualitative value, no experimental points are shown.

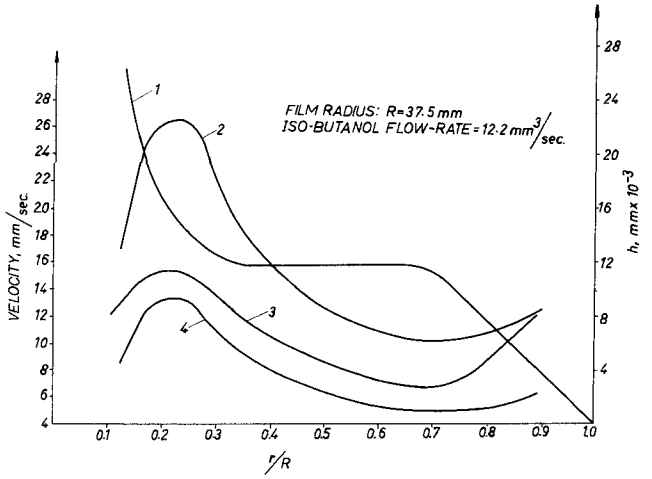

Fig. 6. Comparison between measured and computed velocities, for R = 37.5 mm. 1. Film thickness; 2, 3, 4. film velocities (see text).

film (in degrees probably differing in two successive measurements), its actual velocity will be situated somewhere between that of the film-air interface (maximum film velocity) and that of the film-water interface (minimum velocity).

(b) For film radii in the range of R = 13.5 to 37.5 mm., a translation of the order of 0.1 along the r/R axis (as occurs for instance in (Figure 5), corresponds to effective radial displacements of 1.3 to 3.7 mm., which fall within the observed range of the form fluctuations of the respective circular films.

The period of minute fluctuations of the film is appreciated to be of the order of 1 sec. The time necessary for a tracer to travel along the film radius is of the same order of magnitude, while that necessary to make an extinction reading is ten times longer. This may be considered as an additional explanation for the larger scattering of the experimental points of the film velocity curves, as compared to the film thickness curves.† Besides, one need not overlook the fact that the low response velocity of the mirror galvanometer used during the extinction measurements also smooths out some of the thickness fluctuations.

To be noted is the partial agreement (Figure 6) between the curve giving the velocity computed from the isobutanol film thickness and the corresponding flow-rate, (curve 3), with that (curve 4) obtained by halving the ordinates of the experimental one (curve 2).

In the case where the experimental values (curve 2) represent the actual velocity of the air-film interface, the isobutanol-water interface is stagnant, and the velocity distribution in the film is linear, then curve 4 would correspond to the mean film velocity. The fact that the actual mean velocity (curve 3) lies above the curve 4, may be linked to the fact that the isobutanol-water interface is not stagnant. Indeed, its motion was visualized by injecting colored solution in the vicinity of the film sublayer.

COMMENTS

In analogy to the form of a static drop, and by taking into account the measured thicknesses, one may consider that a cross section through the dissolving film looks like that in Figure 7. The dynamic conditions under which this dynamic drop is existing explain the differences from the static one.

The initial region, up to $r/R \simeq 0.35$ is strongly affected by the capillary forces acting around the capillary tip. The form of the border region, and the contact angle (which is very small) differ in the present case markedly from those of a static drop. The contact angles θ' and θ'' measured for the reciprocally saturated liquids studied here, are of 3 and 42.5 deg. respectively, while the interfacial tensions are $\sigma_{13} = 24.5$, $\sigma_{23} = 2.0$, and $\sigma_{12} = 23$ dynes/cm. (3).

For the static lens the three acting interfacial tensions balance each other:

$$\sigma_{13} = \sigma_{12} \cos \theta' + \sigma_{23} \cos \theta''; \quad \sigma_{12} \sin \theta' = \sigma_{23} \sin \theta''$$

From the experiments presented here, it results that in the dynamic case, the angles θ' and θ'' are very small; therefore the above equations can no longer be satisfied by the static values of the interfacial tensions. A possible assumption is that the dynamic conditions modify these interfacial tensions too, but nevertheless the equilibrium between them is maintained. One may explain the effect of the dynamic conditions as follows:

Owing to the Marangoni effect (4) the interfaces in the vicinity of the border are submitted to extension, and for this reason the dynamic surface tensions are different from the static ones. The value of the border velocity in the film side of the film contour is of the order of magnitude of tens of mm./sec., while that in the free-water side of the contour‡ of the order of hundreds of mm./sec. (both obtained from measured velocities by extrapolating to $r/R = 1$). It results that in the immediate vicinity of the film contour, in the free-water side, there exists a large positive surface velocity gradient. The velocity gradients along the other two interfaces though also positive are smaller.

The gradient of velocity leads to an increase of the interfacial tensions having the same direction with it (that is, σ_{13}) and to a decrease of those having the opposite one (that is, σ_{12} and σ_{23}). In order that the above equalities remain valid it is necessary that the angles θ' and θ'' be smaller than in the static case. In this manner it is possible to explain the smaller angles obtained experimentally for the dynamic lens.

Concerning the radial velocity distribution in the film, we note here only the fact that the surface forces have an effect in the initial region (which is under the action of the capillary) and in the border region. In the middle region, their effect is negligible (therefore h is independent on r) and the average velocity (defined over the thickness of the film) is proportional to $1/r$.

At the end it may be noted the surprising high stability of such thin films, having a R/h ratio of the order of 10^4.

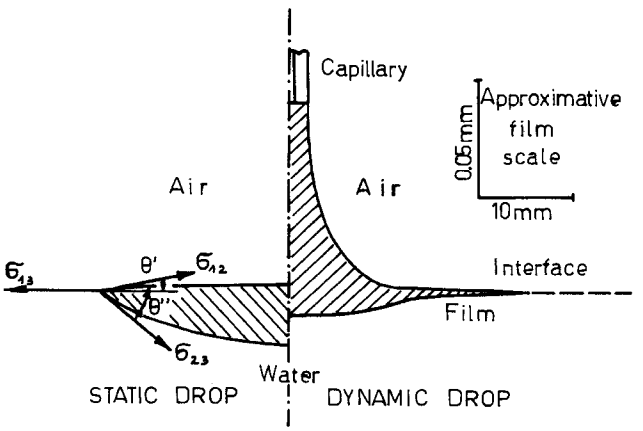

Fig. 7. Cross section through the liquid film.

† Each point plotted on these curves represents an average of 2 to 3 measurements, these did not differ from each other by more than 10%.

‡ The velocity outside the film was measured by using the same technique as above. (Results pertaining to work in progress.)

ACKNOWLEDGMENT

The authors are indebted to Dr. Mihai Elian and Dr. Kalman Ondrejcsik for valuable advice.

NOTATION

h = film thickness, mm.
Q = flow-rate, cc./sec.
r = distance along the film radius
R = film radius, mm.
v = radial velocity, mm./sec.
$\sigma_{12}, \sigma_{13}, \sigma_{23}$ = interfacial tensions (see Figure 7)
$\theta, \theta', \theta''$ = angles as shown in Figure 7; $\theta = \theta' + \theta''$

LITERATURE CITED

1. Suciu, D. G., Octavian Smigelschi, and Eli Ruckenstein, *AIChE J.*, 13, 1120 (1967).
2. ———, D. Eng. thesis, Polytechnical Inst., Bucharest, Romania (1968).
3. Fuchs, V. N., *Koll. Zeit.*, 52, 262 (1930).
4. Scriven, L. E., and Sternling C. V., *Nature*, 187, 186 (1960).

Manuscript received December 26, 1967; revision received April 15, 1968; paper accepted May 13, 1968.

Prediction of Jet Length in Immiscible Liquid Systems

BERNARD J. MEISTER and GEORGE F. SCHEELE

Cornell University, Ithaca, New York

The stability theory is used to predict jet length from jet inception to disruption for injection of one Newtonian liquid into a second immiscible Newtonian liquid. Knowledge of the length is essential for predicting the size of drops formed from jets. At low velocities jet length is controlled by the amplification of symmetrical waves which travel at the interfacial velocity of the jet. At higher velocities an abrupt lengthening of the jet may occur as a result of drop merging, and the jet length is then controlled by the growth rate of sinuous waves which are strongly velocity dependent. Jet disruption results from a geometrical limitation on the maximum amplitude of the sinuous waves. Predictions show good quantitative agreement with experimental data for thirteen mutually saturated systems over a wide range of variables and qualitative agreement with limited experimental data on the effects of initial disturbance level and mass transfer.

When a jet of liquid issues from a nozzle into a second immiscible liquid, the jet attains a length characteristic of the nozzle, injection velocity and physical properties of the liquids. Knowledge of the jet length is important primarily for the prediction of the size of drops formed from jets.

Smith and Moss (*26*) were the first to critically investigate the length of jets. They studied the jetting of liquids into air and derived an equation to predict jet length in the region where the length increases linearly with nozzle velocity. By recognizing that the jet length, L, is the length required for a disturbance to amplify to the magnitude of the jet radius, they obtained the equation

$$L = \frac{U_N}{\alpha} \ln\left(\frac{a_N}{\xi_0}\right) \qquad (1)$$

where α is the growth rate and ξ_0 is the initial amplitude of the most unstable symmetrical disturbance. Equation (1) assumes that the velocity and diameter of the jet are constant and equal to the average nozzle velocity and diameter. Substitution of Rayleigh's equation for α for injection of an inviscid liquid jet into a gas (*21*), and treatment of the quantity a_N/ξ_0 as a constant yields

$$\frac{L}{D_N} = K' N_{We}^{1/2} \qquad (2a)$$

where D_N is the nozzle or orifice diameter.

The data of Smith and Moss, Merrington and Richardson (*17*), Tyler and Richardson (*29*), and Tyler and Watkin (*30*) for low viscosity jets in air satisfy Equation (*2a*), although the constant K' varies from 11 to 16 in the several studies. This is not unexpected because the initial disturbance amplitude is probably a function of the experimental apparatus. Merrington and Richardson found that K' increased with increasing jet viscosity to a value of 84 for a 1,000 centipoise glycerine jet in air. The disturbance growth rate becomes much smaller for very viscous liquids, as shown by Weber's analysis (*33*), and the apparently high value of the constant results from the use of the Rayleigh equation for α in Equation (*2a*). If Weber's analysis for α is used, Equation (1) becomes

$$\frac{L}{D_N} = K' (N_{We}^{1/2} + 3 N_{We}/N_{Re}) \qquad (2b)$$

The data of both Haenlein (*8*) and Merrington and Richardson for viscous liquids show good agreement with Equation (*2b*), with values of $\ln(a_N/\xi_0)$ corresponding to those found from Equation (*2a*) for low viscosity jets.

Several experimental investigations (*12, 15, 24, 25, 30*) of the length of liquid jets in immiscible liquid systems have been made, but agreement with Equation (1) is not necessarily good in the linear region even when the appropriate values for α given by Meister and Scheele (*16*) are employed.

In both liquid-gas and liquid-liquid systems, the jet length-nozzle velocity curve displays a maximum. In liquid-gas systems, this maximum is generally very sharp and is followed immediately by jet disruption, which is characterized by the appearance of random waves, a broad drop size distribution and a sharp decrease in jet length. If

Bernard J. Meister is with The Dow Chemical Company, Midland, Michigan.